three axes have different π-acceptor abilities. Again axes with lower π-acceptor ability will present preferential labilization, and within an axis the weakest π-back-bonding ligand would be preferentially labilized. Assuming that the π-acceptor ability (and the synergistically increased σ-bonding) of the unsaturated ligands follows the order 4-pic < py < isn ≃ pz < 4-acpy, as indicated by the decreasing MLCT transition energy, this is the axes order of π-acceptor ability, and one can see that in a specific complex the ligand aquated with higher quantum yield, or preferentially, is the one that has the lower π-back-bonding ability.

Acknowledgment. This work was supported in part by grants from the CNPq and FAPESP. E.T. acknowledges a research fellowship from the CNPq. L.A.P. acknowledges a doctoral fellowship from the FAPESP and a financial support from the CAPES. We thank Dr. F. A. Leone and the Instituto de Química de Araraquara, UNESP, for the use of their spectrophotometers. We are greatly indebted to Dr. P. C. Ford for helpful discussions, suggestions, and revision of the manuscript.

Registry No. *cis*-$Ru(NH_3)_4(isn)(4\text{-pic})^{2+}$, 132046-85-6; *cis*-$Ru(NH_3)_4(isn)(py)^{2+}$, 60208-54-0; *cis*-$Ru(NH_3)_4(4\text{-acpy})(isn)^{2+}$, 98858-90-3; *cis*-$Ru(NH_3)_4(isn)(pz)^{2+}$, 98858-93-6; *cis*-$Ru(NH_3)_4(4\text{-acpy})_2^{2+}$, 132203-17-9; *cis*-$Ru(NH_3)_4(4\text{-pic})_2^{2+}$, 132046-86-7; *cis*-$Ru(NH_3)_4(py)_2^{2+}$, 46751-30-8; *cis*-$Ru(NH_3)_4(isn)_2^{2+}$, 50573-21-2; *cis*-$Ru(NH_3)_4(pz)_2^{2+}$, 34383-37-4; *trans*-$Ru(NH_3)_4(4\text{-acpy})_2^{2+}$, 115912-47-5; *trans*-$Ru(NH_3)_4(pz)_2^{2+}$, 46751-29-5; *trans*-$Ru(NH_3)_4(pzH)_2^{4+}$, 132046-87-8; *trans*-$Ru(NH_3)_4(isn)(pz)^{2+}$, 60168-50-5; $Ru(NH_3)_5(4\text{-pic})^{2+}$, 19471-55-7; $Ru(NH_3)_5(pz)^{2+}$, 19471-65-9; $Ru(NH_3)_5(pzH)^{3+}$, 19441-21-5; $Ru(NH_3)_5(4\text{-acpy})^{2+}$, 52544-51-1; $Ru(NH_3)_5(isn)^{2+}$, 19471-53-5; $Ru(NH_3)_5(py)^{2+}$, 21360-09-8.

Contribution from the Department of Chemistry, University of Alberta, Edmonton, Alberta, Canada T6G 2G2

Kinetic and Equilibrium Studies of Complexes of Aqueous Iron(III) and Squaric Acid

M. J. Sisley and R. B. Jordan*

Received June 11, 1990

The kinetics and equilibria for the system of aqueous iron(III) and squaric acid (3,4-dihydroxy-3-cyclobutene-1,2-dione) (H_2Sq) have been studied in 1.00 M $HClO_4/LiClO_4$ with concentration ranges of H^+ 0.02–0.10 M, total iron(III) (2.0–7.6) × 10^{-3} M, and total squarate (0.5–2.0) × 10^{-4} M. Spectrophotometric observations lead to the conclusion that two complexes are formed, described by the following reactions with equilibrium constants of 21.4 ± 3.3 and (2.4 ± 0.9) × 10^2 respectively at 23 ± 1 °C: $Fe(OH_2)_6^{3+} + HSq^- \rightleftarrows Fe(OH_2)_5(Sq)^+ + H^+ + H_2O$; $(H_2O)_8Fe_2(OH)_2^{4+} + HSq^- \rightleftarrows (H_2O)_6Fe_2(OH)_2(Sq)^{2+} + H^+ + 2H_2O$. Formation of the iron dimer squarate complex causes the color of solutions to change from bluish purple to bluish red with an absorbance maximum shift from ~540 to lower wavelength as the iron(III) concentration is increased and/or the acidity is decreased. The kinetic observations (25.0 ± 0.1 °C) show a monophasic absorbance change at 545 nm, but a biphasic change at 460 nm, with a 3–5 times larger rate observed at 460 nm. These features are attributed to the formation of the monomeric and dimeric squarate complexes, with rate constants of 5 × 10^4 M^{-1} s^{-1} for $Fe(OH_2)_5OH^{2+} + HSq^-$ or $Fe(OH_2)_6^{3+} + Sq^{2-}$ and 4.5 × 10^4 M^{-1} s^{-1} for $(H_2O)_8Fe_2(OH)_2^{4+} + HSq^-$.

Introduction

Squaric acid (3,4-dihydroxy-3-cyclobutene-1,2-dione, I) is a moderately strong acid ($K_{a1} \approx 0.4$, $K_{a2} = 1.58 \times 10^{-3}$ M)[1] that has some structural analogy to oxalic acid (II) and possibly to ascorbic acid (III). Recent structural studies[2] indicate that

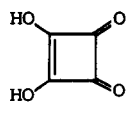

I

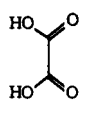

II

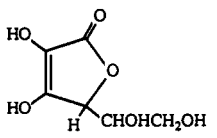

III

squarate forms monodentate complexes and 1,3-bis(metal) complexes rather than 1,2-bidentate chelates with first-row transition metal ions. Solans et al.[2] suggested that squarate does not chelate because of its larger bite distance compared to that of oxalate. A 1,2-bismonodentate structure is found[3] with the bis(μ-hydroxy) dimer of chromium(III), in which squarate acts as a bridge between the two chromium ions. This structure may be especially relevant to the iron(III) chemistry reported here. The analogy to ascorbate with regard to redox properties, has been investigated with pentaammineruthenium(III) complexes.[4]

Tedesco and Walton[1] found that a blue complex is formed in the iron(III)–squaric acid system and that the complex formation can be represented by eq 1, with $K_{f1} \approx 45$ ([iron(III)] ≥ [total squarate] at pH 1.0–1.5). Tedesco and Walton also observed a

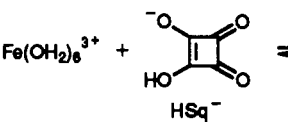

(1)

slow fading of the color, which they attributed to oxidation of squarate, and they noted qualitatively that iron(II) inhibits this reaction.

In many ways, the squarate–iron(III) system is analogous to the ascorbate–iron(III) system. Both form a blue complex whose oxidation is inhibited by iron(II).[5] However, the oxidation with squarate is much slower. Recent work[5] has shown that the initial complexation of ascorbic acid by iron(III) is unusually fast, and this study of the squarate system has been undertaken to seek some explanation for the kinetic observations with ascorbate. It has been found that squarate is unusual in showing clear evidence for complexation with the bis(μ-hydroxy) iron(III) dimer. This product is confirmed by further spectrophotometric studies which reveal that eq 1 does not provide a full representation of the iron(III)–squarate system. In addition, the oxidation stage has been examined in somewhat more detail.

Results

The evolution of our understanding of this system has depended on the interdependence of the stopped-flow and equilibrium

(1) Tedesco, P. H.; Walton, H. F. *Inorg. Chem.* **1969**, *8*, 932.
(2) Solans, X.; Aguiló, M.; Gleizes, A.; Faus, J.; Julve, M. *Inorg. Chem.* **1990**, *29*, 775 and references therein.
(3) Chesick, J. P.; Doany, A. F *Acta Crystallogr.* **1981**, *B37*, 1076.
(4) Bryan, D. M.; Pell, S. D.; Kumar, R.; Clarke, M. J.; Rodriguez, V.; Sherban, M.; Charkoudian, J. *J. Am. Chem. Soc.* **1988**, *110*, 1498.
(5) Xu, J.-H.; Jordan, R. B. *Inorg. Chem.* **1990**, *29*, 4180.

0020-1669/91/1330-2190$02.50/0

spectrophotometric observations. All of the results pertain to solutions containing excess iron(III) ((1–4) × 10^{-3} M) compared to squaric acid ((0.5–2.0) × 10^{-4} M). Preliminary stopped-flow results showed that the complex formation reaction, observed at 545 nm, is biphasic for $[H^+] \leq 0.02$ M. The biphasic behavior can be induced at higher final acidities when an iron(III) solution at lower acidity is mixed with squarate at higher acidity to give an intermediate final acidity (e.g. iron(III), squarate, and final acidities of 0.020, 0.080, and 0.050 M, respectively). This observation implicates the bis(μ-hydroxy) iron(III) dimer because dissociation of the dimer is slow[6,7] relative to the complexation and it will have a higher concentration in the iron(III) stock solution at lower acidity before mixing, compared to the normal case of mixing solutions of equal acidities.

These observations led us to reexamine the equilibrium system. The results of Tedesco and Walton[1] at 545 nm were confirmed. However, there is another chromophore in the system with an absorbance maximum in the 460-nm region (based on a Gaussian line shape analysis of the equilibrium results described below). This species is favored by lower acidity and higher iron(III) concentrations and produces a change in color from blue-purple to red-purple. It appears that the biphasic kinetic behavior is associated with the formation of these two species. This was confirmed by stopped-flow experiments which showed that biphasic character is observed under a much wider range of conditions at 460 nm than at 545 nm.

Oxidation of Squarate by Aqueous Iron(III). We have confirmed the observation of Tedesco and Walton[1] that the color of iron(III)–squarate solutions fades significantly over a period of a few hours and that the fading is inhibited by aqueous iron(II). For a solution initially containing 1.93 × 10^{-3} M iron(III) and 6.04 × 10^{-4} M squaric acid in 0.05 M H^+ and exposed to air, the absorbance decreases by 24% (1.64 to 1.25) in 5 min and by 50% in 30 min. If the solution is stored anaerobically, the absorbance decreases by 13% in 150 min, and if 1 × 10^{-3} M iron(II) is present, there is <1% change over this time period. Solutions stored anaerobically for 7 weeks still retain some purple color. Clearly, the oxidation process is inhibited by iron(II), but if the solutions are exposed to air, the iron(II) is oxidized to iron(III) by dioxygen and oxidation proceeds slowly to completion.

It was hoped that the oxidation kinetics might be followed by using 1,10-phenanthroline as a scavenger and spectrophotometric indicator for iron(II). The ionic medium had to be LiCl because of the low solubility of the perchlorate and trifluoromethanesulfonate salts of $Fe(phen)_3^{2+}$. In order to avoid significant amounts of iron(III)–phen complexes, it is necessary to have $[phen] \leq 2 \times 10^{-3}$ M, and then the formation of $Fe(phen)_3^{2+}$ becomes rate controlling and therefore useless as a kinetic monitor under our acidity conditions. Nevertheless, the spectrophotometric observations show that 1,10-phenanthroline increases the amount of oxidation in a given time period, presumably by removing the $Fe(OH_2)_6^{2+}$ inhibitor.

It was found that cyclobutaneoctol, the probable two-electron-oxidation product of squarate,[8] is oxidized within 5 min by iron(III) under our conditions, while oxalate is ≤5% oxidized after 2 h. Therefore oxalate would seem to be the dominant product of the oxidation of squarate at least after a few hours at ambient temperature.

Spectrophotometric Equilibrium Studies. This work was done at ambient temperature (23 ± 1 °C) on a Hewlett-Packard diode array spectrophotometer, which allows us to measure the spectrum over a suitable wavelength range within 30 s after mixing the solutions. The time is of some importance because of the oxidation step that follows the complexation, but the absorbance is constant within experimental error (±0.002 unit) for at least 60 s. The total iron(III) concentration was at least 10 times larger than the total squarate to avoid bis(squarate) complexes. Details are given in the Experimental Section.

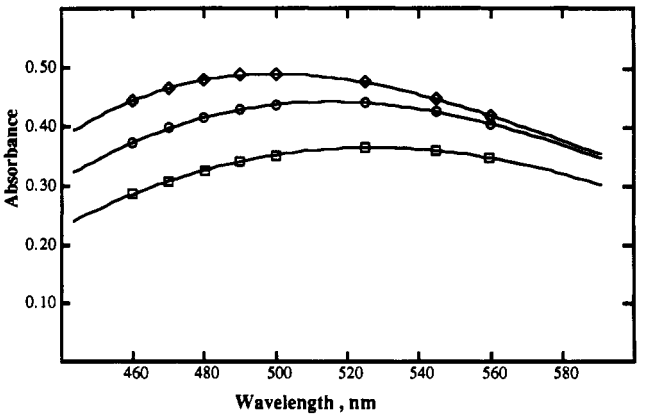

Figure 1. Variation of absorbance with wavelength for solutions of iron(III) and squaric acid (2.02 × 10^{-4} M) in 0.020 M $HClO_4$/0.98 M $LiClO_4$: 2.00 × 10^{-3} M Fe(III) (□); 4.01 × 10^{-3} M Fe(III) (○); 7.56 × 10^{-3} M Fe(III) (◇).

The absorbance increases with increasing [Fe(III)] and/or decreasing $[H^+]$, as would be expected if the system is represented by eq 1. However, the absorbance maximum also shifts to shorter wavelength as the [Fe(III)] increases, as shown in Figure 1. Since Fe(III) is in excess, this behavior indicates the formation of a second complex that contains more than one Fe(III) per squarate and has an absorbance maximum in the 460-nm region, compared to ~550 nm for the mono(squarato)iron(III) complex.

There are several possible dimeric complexes on the basis of previous structural studies[2,3] with other metal ions. These possibilities are described by eqs 2–4. The product in eq 2 could

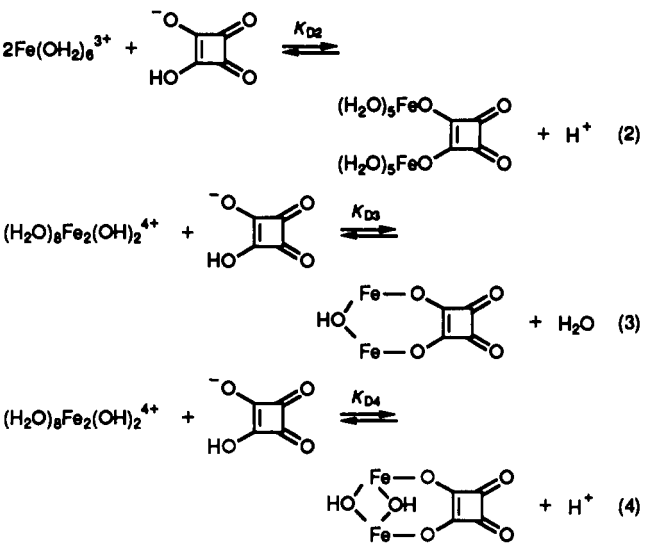

involve 1,3-coordination to squarate. However, eq 2 will not explain why more of the dimer, relative to monomer, is formed at lower $[H^+]$, since eqs 1 and 2 involve the same number of protons released relative to $Fe(OH_2)_6^{3+}$ and Hsq^-. In eq 3, the reactant is the bis(μ-hydroxy) dimer of iron(III) and the product is a μ-hydroxy-μ-squarato dimer. The coordinated water ligands have been omitted in the product for clarity, but it is intended that the iron(III) is six-coordinate. The process in eq 3 involves the release of one more proton than eq 1, because of one proton per iron(III) to form $(H_2O)_8Fe_2(OH)_2^{4+}$, so that eq 3 would predict more dimer complex at lower acidity. The product in eq 4 is the direct analogue of the chromium(III) squarate dimer.[3] The reaction involves the release of one more proton than eq 3.

The dependence of the absorbance on [Fe(III)] and $[H^+]$ at eight wavelengths between 460 and 560 nm has been fitted to the two models defined by eq 1 plus eq 4 (model I) or eq 1 plus eq 3 (model II). The details of the fitting process are described in the Experimental Section. Model I provides a better fit of the data with an overall standard error 2 times smaller than that for

(6) Sommer, B. A.; Margerum, D. W. *Inorg. Chem.* **1970**, *9*, 2517.
(7) Po, H. N.; Sutin, N. *Inorg. Chem.* **1971**, *10*, 428.
(8) West, R.; Niu, H. Y.; Ito, M. *J. Am. Chem. Soc.* **1963**, *85*, 2584.

model II. For model I, only 6 of the 72 calculated data points deviate by more than 0.01 absorbance unit from the observed value, with a maximum deviation of 0.015. For model II, 24 points deviate by more than 0.01, with a maximum deviation of 0.025. Neither model shows any systematic pattern of deviations between the observed and calculated values. Both models yield K_{fl} values close to 20 and similar values for the molar absorptivities.[9]

The reasons for preferring model I are (i) it provides a better fit of the absorbance data, (ii) the product of eq 4 has a well-established precedent in its chromium(III) analogue,[3] (iii) there is no apparent reason why squarate complexation should break one μ-hydroxy bridge in eq 3, and (iv) the equilibrium constants are consistent with the kinetic observations described in the following section. The best fit to model I gives $K_{fl} = 21.4 \pm 3.3$ (eq 1) and $K_{D4}K_{DFe} = 0.45 \pm 0.17$, where $K_{DFe} = 1.9 \times 10^{-3}$ M[10] is the equilibrium constant for eq 5, so that $K_{D4} = (2.4 \pm 0.9) \times 10^2$.

$$2Fe(OH_2)_6^{3+} \overset{K_{DFe}}{\rightleftharpoons} (H_2O)_8Fe_2(OH)_2^{4+} + 2H^+ \quad (5)$$

Stopped-Flow Kinetic Studies. The absorbance–time curves at 545 nm appear monophasic at 0.05 M H^+ but are distinctly biphasic at 0.02 M H^+ and at an iron(III) solution acidity <0.02 M before mixing with a more acidic solution of squaric acid. The biphasic nature is apparent under all conditions at 460 nm, and the rate of the absorbance change is larger at 460 nm. These observations, when combined with those of the equilibrium study, suggest that the two kinetic phases are associated with formation of the products in eqs 1 and 4. The product of the latter reaction is favored at lower acidity and has the higher absorbance around 460 nm. It is known[6,7] that formation and dissociation of the bis(μ-hydroxy) iron(III) dimer (eq 5) occur on the seconds time scale, and our own observations at 460 nm show that the absorbance change associated with eq 5 is <10% of that observed in the presence of squarate. Therefore dissociation of the bis(μ-hydroxy) iron(III) dimer is not the source of the biphasic behavior.

The involvement of the bis(μ-hydroxy) iron(III) dimer presents a complication with regard to the concentrations of the aquairon(III) reactants. Before mixing on the stopped-flow system, the equilibrium dimer concentration can be calculated in a standard way from the total iron(III). After mixing, the total iron(III) concentration is reduced by half but the equilibrium described by eq 5 is established more slowly than the complexation. Therefore, the dimer concentration will just be half of its value in the iron(III) stock solution before mixing, but the $Fe(OH_2)_6^{3+}/Fe(OH_2)_5(OH)^{2+}$ equilibrium will be rapidly established relative to the complexation. This effect has been taken into account in the analysis of the kinetic results.

The increase in absorbance at 545 nm can be attributed primarily to formation of the monomeric complex (eq 1) because the molar absorbance of the dimeric product[9] is 32% of that of the monomer at this wavelength and the dimer is <25% of the total complex formed. Therefore these data can be analyzed in the usual way for complexation of aqueous iron(III). The results are consistent with complexation by either or both of the pathways shown in eqs 6 and 7. This predicts that the pseudo-first-order

$$Fe(OH_2)_5(OH)^{2+} + HSq^- \underset{k_{-6}}{\overset{k_6}{\rightleftharpoons}} Fe(OH_2)_5(Sq)^+ + H_2O \quad (6)$$

$$Fe(OH_2)_6^{3+} + Sq^{2-} \underset{k_{-7}}{\overset{k_7}{\rightleftharpoons}} Fe(OH_2)_5(Sq)^+ + H_2O \quad (7)$$

rate constant will be given by eq 8, where $[Fe]_{mono}$ is ($[Fe(OH_2)_6^{3+}]$ + $[Fe(OH_2)_5(OH)^{2+}]$), K_m is the hydrolysis constant of $Fe(OH_2)_6^{3+}$ (1.62×10^{-3} M),[10] and K_{a1} and K_{a2} are the first and second acid dissociation constants of squaric acid. A least-squares analysis gives $(k_6K_m + k_7K_{a2}) = 81 \pm 6$ s^{-1} and $K_{fl} = 18 \pm 7$. The latter is in good agreement with the value of 21.4 from the equilibrium studies.[11] The observed and calculated rate constants are compared in Table I. Since K_m and K_{a2} are almost identical, one can calculate that $k_1' = (k_6 + k_7) = (5 \pm 0.4) \times 10^4$ M^{-1} s^{-1}.

$$k_{obsd} = (k_6K_m + k_7K_{a2})\left\{\left(\frac{[Fe]_{mono}}{K_m + [H^+]}\right) \times \left(\frac{K_{a1}[H^+]}{[H^+]^2 + K_{a1}[H^+] + K_{a1}K_{a2}}\right) + \frac{1}{K_{fl}}\right\} \quad (8)$$

Table I. Rate Constants for the Reaction of Aqueous Iron(III) and Squaric Acid,[a] Observed at 545 nm in 1.00 M $LiClO_4/HClO_4$ at 25.0 °C

10^3[Fe(III)], M	$10^2[H^+]_i$, M	$10^2[H^+]_f$, M	k_{obsd}, s^{-1} obsd	k_{obsd}, s^{-1} calcd[b]
2.01	2.02	2.05	11.1	10.9
2.99	2.04	2.09	13.4	13.7
4.01	2.02	2.095	17.95	16.6
2.01	5.01	5.09	8.67	9.81
1.03	9.98	9.98	5.06	5.17
2.01	10.0	10.0	5.84	5.79
4.00	10.0	10.0	7.56	7.04
4.00	10.0	10.0	7.66[c]	7.04

[a] The total squarate concentration is 1.0×10^{-4} M unless otherwise indicated. [b] Calculated from a least-squares fit to eq 8. [c] The total squarate concentration is 0.51×10^{-4} M.

The absorbance increase observed at 460 nm is 3–10 times faster than that at 545 nm and shows clear biphasic behavior under most conditions. Since the dimeric squarate complex has about a 2 times larger molar absorptivity[9] than the monomer at 460 nm, the faster rate observed at 460 nm can be qualitatively ascribed to dimer complex formation. However, the dimer concentration is often 2–5 times less than the monomer, so that monomer still makes a significant contribution to the overall absorbance change at 460 nm. The system is further complicated because the concentration of the bis(μ-hydroxy) iron(III) reactant is in the same range as that of the squarate anion, so that the conditions for the dimer complex formation are second order. Thus, we have numerically integrated the differential equations based on the reactions in Scheme I to calculate the concentrations of the iron complexes to describe the kinetic observations at 460 nm. The last reaction in Scheme I is included because the initial amount of bis(μ-hydroxy) dimer after mixing depends on the iron(III) in the stock solution before mixing. Therefore, the bis(μ-hydroxy)–squarate complex formed in step k_4 may dissociate directly to an equilibrium concentration related to the total iron(III) after mixing. The monomer–dimer reaction (eq 5) was also included in the model using the kinetic parameters determined by Sommer and Margerum,[6] but this reaction has very little effect on the 100–500-ms time scale of our observations.

Scheme I

$$Fe(OH_2)_5(OH)^{2+} + HSq^- \underset{k_{-1'}}{\overset{k_1'}{\rightleftharpoons}} Fe(OH_2)_5(Sq)^+ + H_2O$$

$$(H_2O)_8Fe_2(OH)_2^{4+} + HSq^- \underset{k_{-4}}{\overset{k_4}{\rightleftharpoons}} (H_2O)_6Fe_2(OH)_2(Sq)^{2+} + 2H_2O + H^+$$

$$(H_2O)_6Fe_2(OH)_2(Sq)^{2+} + H^+ \underset{k_{-5}}{\overset{k_5}{\rightleftharpoons}} Fe(OH_2)_5(Sq)^+ + Fe(OH_2)_5(OH)^{2+}$$

(9) Model I gives values of the molar absorptivity ($10^{-3}\epsilon$, M^{-1} cm^{-1}) at 560, 545, 525, 500, 490, 480, 470, and 460 nm, respectively: for $Fe(Sq)^+$, 1.98, 1.99, 1.92, 1.74, 1.61, 1.51, 1.36, and 1.22; for $(HO)_2Fe_2(Sq)^{2+}$, 0.17, 0.63, 1.33, 2.16, 2.50, 2.71, 2.92, and 2.06. For Model II, the corresponding values are as follows: for $Fe(Sq)^+$, 1.90, 1.99, 1.91, 1.70, 1.58, 1.45, 1.30, 1.17, and 1.17; for $(HO)_2Fe_2(Sq)^{2+}$, 0.43, 0.78, 1.40, 2.20, 2.46, 2.70, 2.89, and 2.83. The values of K_{fl} and $K_{D3}K_{DFe}$ are 21.4 ± 8.5 and 22.1 ± 23, respectively.

(10) Baes, C. F.; Messmer, R. E. *The Hydrolysis of Cations*; Wiley: New York, 1976; Chapter 10.5. Milburn, R. M.; Vosburgh, W. C. *J. Am. Chem. Soc.* **1955**, *77*, 1352.

(11) The overall standard error of the fit is improved by 3% if the reactions of $Fe(OH)^{2+} + H_2Sq$ (k_2) and $Fe(OH_2)^{3+} + HSq^-$ (k_3) are included, but the additional term in eq 8 of $(k_2K_m/K_{a1}) + k_3 = (1.5 \pm 1.6) \times 10^2$ M^{-1} s^{-1} is not defined relative to its standard error.

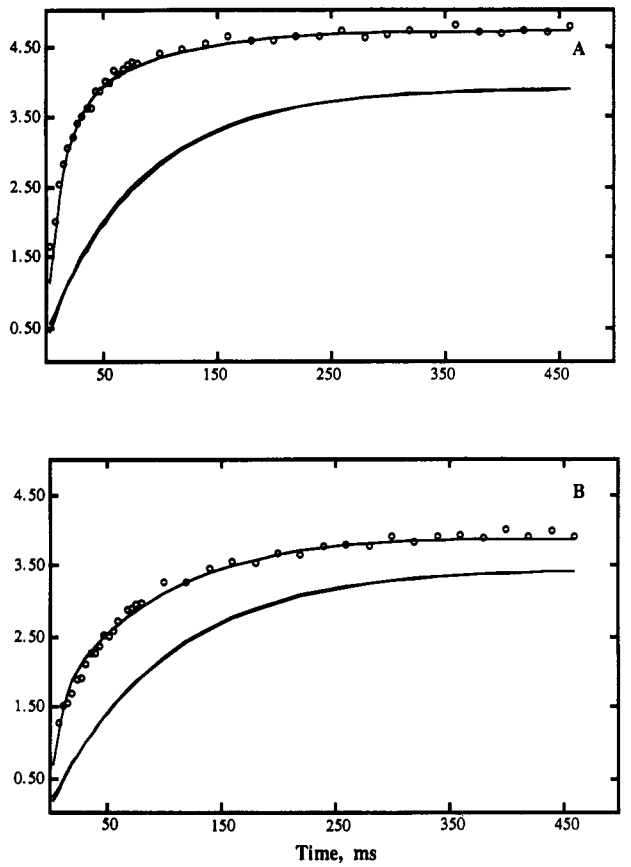

Figure 2. Variation of absorbance with time: (A) 1.94×10^{-3} M Fe(III), 2.04×10^{-2} M H^+, and 1.0×10^{-4} M total squarate at 460 nm (O); (B) 2.96×10^{-3} M Fe(III), 4.03×10^{-2} M H^+, and 1.0×10^{-4} M total squarate at 460 nm (O). The curves are calculated on the basis of the reactions in Scheme I. The lower curves in each panel are a single-exponential curve with a rate constant predicted by eq 8 and the curve predicted at 545 nm from Scheme I.

The rate constants in Scheme I were determined by graphical comparison of the observed time dependence of the absorbance at 460 nm to that calculated by numerical integration from Scheme I. The forward rate constants were varied to obtain a graphical fit, with the reverse rate constants determined from the ratio of the forward constants and the known equilibrium constants. The molar absorptivities for the iron(III)–squarate complexes were taken from the equilibrium measurements.[9] Three criteria were used to determine satisfactory rate constants: the results must give a reasonable representation of the absorbance–time curves at 460 nm; the predicted change at 545 nm must be a reasonable simple exponential curve; the time constant for the change at 545 nm must be consistent with the predictions from eq 8. Some representative results are shown in Figures 2 and 3, where the calculated absorbance change at 545 nm is given also. These runs demonstrate the different types of behavior observed at 460 nm. Figure 2A shows almost single-exponential behavior, but the rate constant is about 5 times greater than that at 545 nm. Qualitatively, this is because dimer complex formation is the dominant observable process at lower acidity. In Figure 2B, the absorbance change is clearly not simple first order because the slower formation of the monomer complex contributes significantly at the higher acidity. Similar behavior is seen in Figure 3A, except that the reaction is faster because of the higher iron(III) and lower H^+ concentrations compared to the case of Figure 2B. In Figure 3B, there is a significant decrease in absorbance after about 25 ms, which is due to the k_5 step in Scheme I. This step becomes important at the lower acidities and higher iron(III) concentrations because of the greater relative importance of the dimeric species. The calculated curves at 545 nm in Figure 2 are indistinguishable from those predicted by eq 8. In Figure 3, the calculated curves at 545 nm show a more rapid increase up to about 15 ms before matching the curve from eq 8 for the rest of the reaction. It is not surprising that this small fast stage would be overlooked in a typical routine analysis of such data. As expected, the observations at 545 nm are essentially controlled by the value of k_1' ($=k_6 + k_7$).

The results at 545 nm in Figure 4 show the effect of having the iron(III) solution at a lower acidity before mixing with squarate at a higher acidity to give a final $[H^+] = 0.050$ M. If the solutions are both 0.050 M in H^+, there is a monophasic increase in absorbance at 545 nm. The iron solutions initially at lower acidity will contain more of the bis(μ-hydroxy) iron(III) dimer, and our model predicts that biphasic behavior then should be observable at 545 nm.

The overall results are consistent with $k_1' = (5 \pm 1) \times 10^4$ M^{-1} s^{-1}, as determined at 545 nm, $k_4 = 4.5 \times 10^5$ M^{-1} s^{-1}, and $k_5 = 3 \times 10^3$ M^{-1} s^{-1}. It is difficult to assign uncertainties to the latter two values because their importance varies with the conditions and the values given are based on an overall perspective of the adequacy of the graphical comparisons. However, variations in the values beyond the 20% level produce less than satisfactory fits under certain conditions.

Discussion

The coordination chemistry of squarate with first-row transition-metal ions has been summarized recently by Solans et al.[2] They conclude that squarate is probably monodentate in these systems because the bite distance of 3.3 Å between the adjacent oxygens is too long to accommodate chelate formation. This distance is about 2.6 Å for chelating ligands such as oxalate. Several solid M(III) complexes of the general formula $(M(Sq)(OH)(H_2O)_2)_2$ have been prepared[8,12,13] with the suggested dimeric structure IV, although this violates the suggestion of only

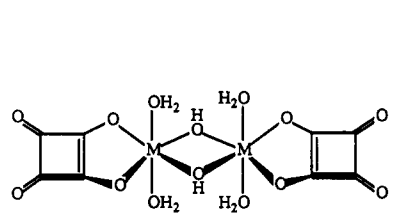

IV

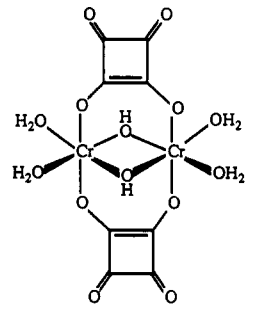

V

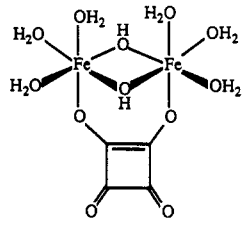

VI

monodentate complexation for squarate. Chesick and Doany[3] found that the structure of a chromium(III) dimer is as shown in V. Therefore, the previously prepared M(III) complexes may have a bis(μ-squarato)–bis(μ-hydroxo) structure with the squarate monodentate on a particular metal ion, but the long bite distance allows the ligand to bridge between two metal centers. These observations suggest that the monomeric iron(III)–squarate complex is probably monodentate $(H_2O)_5Fe(Sq)^+$, while the dimeric iron(III) complex has structure VI.

In principle, the complex formation constant for $Fe(Sq)^+$ could provide some evidence as to whether the squarate is monodentate, but it is difficult to find reasonably analogous systems for com-

(12) Wrobleski, J. T.; Brown, D. B. *Inorg. Chem.* **1978**, *17*, 2959.
(13) Condren, S. M.; McDonald, H. O. *Inorg. Chem.* **1973**, *12*, 57.

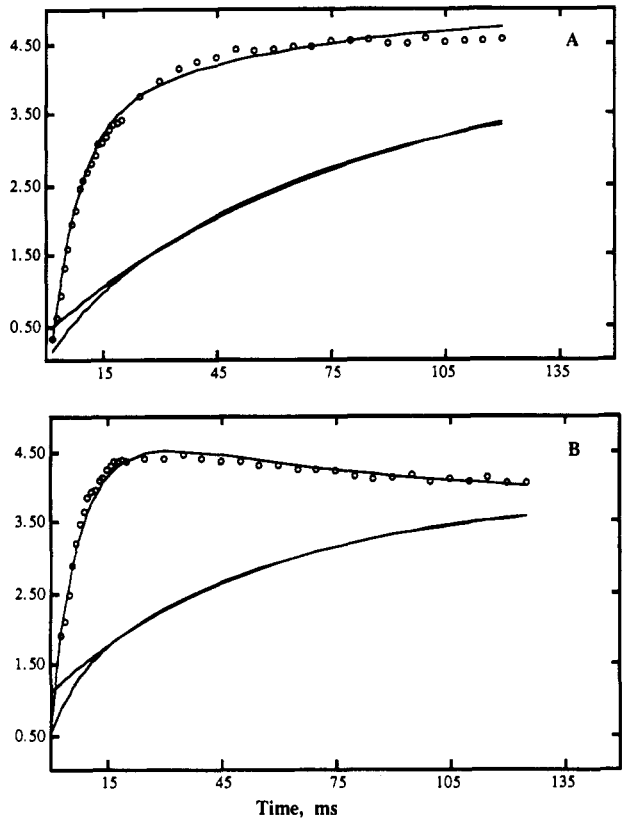

Figure 3. Variation of absorbance with time: (A) 3.89×10^{-3} M Fe(III), 3.04×10^{-2} M H^+, and 2.0×10^{-4} M total squarate at 460 nm (O); (B) 3.80×10^{-3} M Fe(III), 2.08×10^{-2} M H^+, and 1.0×10^{-4} M total squarate at 460 nm (O). The curves are calculated on the basis of the reactions in Scheme I. The lower curves in each panel are a single-exponential curve with a rate constant predicted by eq 8 and the curve predicted at 545 nm from Scheme I.

parison. The formation of the iron(III)–oxalate complex[14] has $\beta_1 = 3.9 \times 10^7$ M, while the analogous value for squarate is $[Fe(Sq)^+]/[Fe(OH_2)^{3+}][Sq^{2-}] = K_{f1}/K_{a2} = 1.3 \times 10^4$ M. These values are consistent with a more stable, bidentate oxalate complex and a squarate monodentate complex.

A determination of whether the k_6 or k_7 path is dominant in the formation of the monomeric complex can only be based on comparisons to other systems. Such comparisons are complicated for the k_7 path because substitution on $Fe(OH_2)_6^{3+}$ is thought to have associative character.[15] Previous results for complexation of $Fe(OH_2)_5(OH)^{2+}$ by $HC_2O_4^-$,[16] the salicylate anion,[17] and other monoanions[18] indicate that k_6 should be in the range $(1–4) \times 10^4$ M^{-1} s^{-1}, so that the value of 5×10^4 for HSq^- is not unreasonable. The only comparable system for k_7 is the reaction of $Fe(OH_2)_6^{3+}$ + SO_4^{2-}, for which $k = 4 \times 10^3$ M^{-1} $1 s^{-1}$.[18] Therefore, a value of $k_7 = 5 \times 10^4$ for $Fe(OH_2)_6^{3+} + Sq^{2+-}$ seems high.

One purpose of this study is to compare the complexation of aqueous iron(III) by ascorbic acid (H_2A)[5] and squaric acid. Ascorbic acid has an unusually large rate constant of 5.5×10^3 M^{-1} s^{-1} for $Fe(OH_2)_6^{3+} + H_2A$. Unfortunately, squaric acid is such a strong acid ($K_{a1} = 0.4$ M) that H_2Sq is a minor species and the $Fe(OH_2)_6^{3+} + H_2Sq$ path could not be detected. It is possible[11] to put an upper limit of $k \leq 7 \times 10^4$ M^{-1} s^{-1} for $Fe(OH)^{2+} + H_2Sq$ and $k \leq 3 \times 10^2$ M^{-1} s^{-1} for $Fe(OH_2)^{3+} + HSq^-$. The former limit is not inconsistent with the possible value[5] of 5×10^4 M^{-1} s^{-1} for $Fe(OH)^{2+} + H_2A$, but the latter value makes the alternative suggestion of 3×10^5 M^{-1} s^{-1} for $Fe(OH_2)^{3+}$ + HA^- seem unreasonable. Therefore, the squaric acid results are of some help in resolving the proton ambiguity problem with ascorbic acid.

An important result of the present work is the identification of complexation of the bis(μ-hydroxy) iron(III) dimer. This species has been inferred as a reactant in some previous work[19,20] based on a term in the rate law with an $[Fe(III)]^2$ dependence. The kinetic results are summarized as follows:

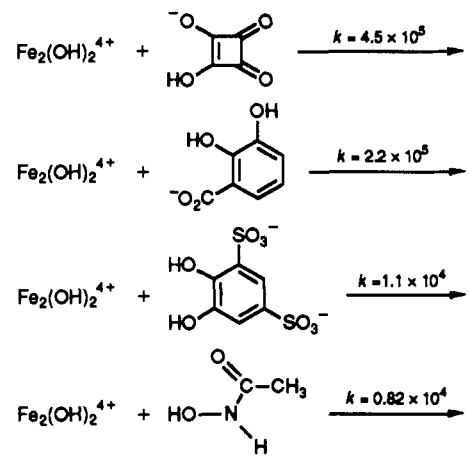

These results show the sensitivity of the rate constant to charge at the reaction site, which is typical for a dissociative ion-pair mechanism.[21] Squarate and dihydroxybenzoate have a uninegative group reacting and similar rate constants, while Tiron has an $-SO_3^-$ group near the neutral reaction site and has a somewhat larger rate constant than neutral acetohydroxamic acid.

Since squarate is thus far unique in forming a stable complex with the bis(μ-hydroxy) iron(III) dimer, there are no literature values to compare to k_5. The acid-catalyzed dissociation of $(H_2O)_8Fe_2(OH)_2^{4+}$ itself[6] has a rate constant of 3.1 M^{-1} s^{-1} at 25 °C, so that the squarate dimer complex dissociates 10^3 times faster than its parent. Acceleration of the dissociation by coordination of Sq^{2-} would be expected on the basis of simple charge neutralization arguments.

Experimental Section

Materials. Solutions of lithium perchlorate, perchloric acid,[22] and iron(III) perchlorate[19] were prepared and standardized as described previously. 3,4-Dihydroxy-3-cyclobutene-1,2-dione (squaric acid) (Aldrich, 99%) was converted to the more soluble dilithium salt by reaction in water with Li_2CO_3, followed by crystallization from water and drying at 10^{-3} mmHg, to yield $Li_2C_4O_4 \cdot 2H_2O$. Lithium squarate was characterized by C and H analysis and its electronic spectrum. The cyclobutaneoctol was prepared by Br_2 oxidation of squaric acid, following the procedure of West and Niu.[8]

Spectrophotometric Equilibrium Constant Determination. The electronic spectra were recorded on a Hewlett-Packard 8451 diode array spectrophotometer between 450 and 600 nm at ambient temperature (23 ± 1 °C). An appropriate amount of a solution of lithium squarate, perchloric acid, and lithium perchlorate was placed in a 1 cm path length spectrophotometer cell, a measured volume of a solution of iron(III) perchlorate in the same medium was added, and the spectrum was recorded as quickly as possible and then at 20-s intervals for 60 s. The absorbance was constant (±0.002 absorbance unit) over the 60-s interval. Nine solutions were studied containing 2.022×10^{-4} M total squarate, 2.00, 4.01, and 7.56 mM total iron(III), and 0.0201, 0.0296, and 0.0496 M $HClO_4$ with $LiClO_4$ added to give an ionic strength of 1.00 M. Absorbance values at 460, 470, 480, 490, 500, 525, 545, and 560 nm for each solution were fitted to models tested. The H^+ concentration was corrected for the H^+ produced by hydrolysis and dimerization of the

(14) Dellien, I. *Acta Chem. Scand.* **1977**, *A31*, 473.
(15) (a) Grant, M.; Jordan, R. B. *Inorg. Chem.* **1981**, *20*, 55. (b) Swaddle, T. W.; Merbach, A. E. *Inorg. Chem.* **1981**, *20*, 4212.
(16) Moorehead, E. G.; Sutin, N. *Inorg. Chem.* **1966**, *5*, 1866.
(17) Jordan, R. B. *Inorg. Chem.* **1983**, *22*, 4160.
(18) Cavasino, F. P. *J. Phys. Chem.* **1968**, *72*, 1378.
(19) Xu, J.; Jordan, R. B. *Inorg. Chem.* **1988**, *27*, 1502.
(20) Birus, M.; Kryundzic, N.; Pribanic, M. *Inorg. Chim. Acta* **1980**, *55*, 65.
(21) Eigen, M.; Wilkins, R. G. *Adv. Chem. Ser.* **1965**, *49*, 55.
(22) Sisley, M.; Jordan, R. B. *Inorg. Chem.* **1987**, *26*, 273.

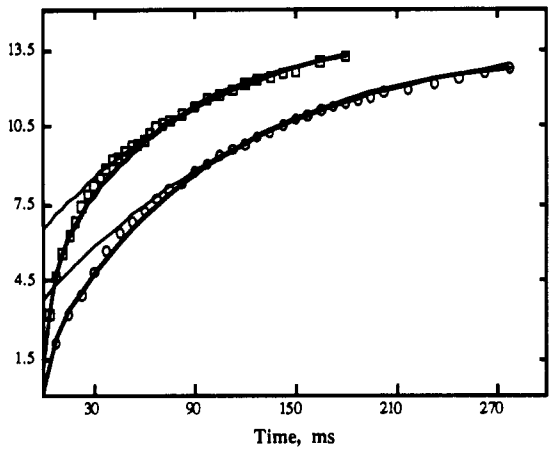

Figure 4. Variation of absorbance with time at 545 nm in 1.0 M $LiClO_4/HClO_4$ at 25 °C for runs with lower $[H^+]$ in the initial iron(III) solution: 4.02×10^{-3} M Fe(III) in 2.02×10^{-2} M H^+ mixed with 1.0×10^{-4} M squarate in 8.02×10^{-2} M H^+ (○); 8.04×10^{-2} M Fe(III) in 2.02×10^{-2} M H^+ mixed with 1.0×10^{-4} M squarate in 8.02×10^{-2} M H^+ (□). The lighter curves represent a first-order time dependence with the rate constants calculated from eq 8.

iron(III). For model I, with [total Fe(III)] ≫ [total squarate] the absorbance (Ab) is given by the following equations:

$$\mathrm{Ab} = (\epsilon_1[\mathrm{FeSq}^+] + \epsilon_2[(\mathrm{HO})_2\mathrm{Fe}_2\mathrm{Sq}^{2+}])l = \left(\epsilon_1 K_{f1} + \frac{\epsilon_2 K_{D4} K_{DFe}[\mathrm{Fe(OH_2)}]}{[\mathrm{H}^+]^2}\right)\left(\frac{[\mathrm{Fe(OH_2)}]}{[\mathrm{H}^+]}\right)\left(\frac{[\mathrm{Sq}]_{tot}}{A+B}\right)l$$

$$A = \left(K_{f1}[\mathrm{H}^+] + \frac{K_{D4}K_{DFe}[\mathrm{Fe(OH_2)}]}{[\mathrm{H}^+]}\right)\left(\frac{[\mathrm{Fe(OH_2)}]}{[\mathrm{H}^+]^2}\right)$$

$$B = \frac{[\mathrm{H}^+]^2 + K_{a1}[\mathrm{H}^+] + K_{a1}K_{a2}}{K_{a1}[\mathrm{H}^+]}$$

Here $[Fe(OH_2)]$ is the concentration of $Fe(OH_2)_6^{3+}$, $[Sq]_{tot}$ is the total squarate concentration, l is the cell path length (1.00 cm), and ϵ_1 and ϵ_2 are the molar absorptivities of the squarate complexes. Similarly, for model II

$$\mathrm{Ab} = (\epsilon_1[\mathrm{FeSq}^+] + \epsilon_2[(\mathrm{HO})\mathrm{Fe}_2\mathrm{Sq}^{3+}])l = \left(\epsilon_1 K_{f1} + \frac{\epsilon_2 K_{D3} K_{DFe}[\mathrm{Fe(OH_2)}]}{[\mathrm{H}^+]}\right)\left(\frac{[\mathrm{Fe(OH_2)}]}{[\mathrm{H}^+]}\right)\left(\frac{[\mathrm{Sq}]_{tot}}{A+B}\right)l$$

$$A = (K_{f1}[\mathrm{H}^+] + K_{D3}K_{DFe}[\mathrm{Fe(OH_2)}])\left(\frac{[\mathrm{Fe(OH_2)}]}{[\mathrm{H}^+]^2}\right)$$

The other symbols are as defined previously. The least-squares fits involve determination of the best values of the two complex formation constants and the two molar absorptivities (at each wavelength) simultaneously at the eight wavelengths.

Stopped-Flow Kinetic Studies. Solutions of aqueous iron(III) perchlorate and lithium squarate were mixed on a Tritech Dynamic Instruments stopped-flow system (Model IIA), and the change of absorbance with time was monitored at 545 or 460 nm. In most cases, the two solutions were identical in the amounts of perchloric acid and lithium perchlorate. Some experiments were done with less perchloric acid initially in the iron(III) stock solution.

The stopped-flow system is of a standard design that mixes equal amounts of two solutions in a glass and Teflon flow and mixing system. The reservoir and drive syringes are in a thermostated water bath with the temperature regulated at 25 ± 1 °C by a YSI thermistor controller. The absorbance–time data are collected and stored digitally on a transient recorder (Tritech Dynamic Instruments, Model 1024) and output to a dual-trace oscilloscope for comparison to a synthetic exponential decay signal for determination of the rate constant. When the observations do not fit a single-exponential curve, the data are output and printed through a digital voltmeter and then fitted to a two-exponential model by nonlinear least squares.

Numerical Analysis. The nonlinear least-squares program uses a Newton–Raphson procedure[23] and has been adapted to run in BASIC on a Macintosh computer. Errors quoted are 95% confidence limits. The fourth-order Runge–Kutta integration uses published algorithms[24] in a program in BASIC.

Acknowledgment. We thank the Natural Sciences and Engineering Research Council of Canada for financial support. We gratefully acknowledge Dr. R. E. D. McClung for assistance with the numerical integration procedure.

(23) Share No. SDA 3094, IBM 360–65.
(24) Romanelli, M. J. In *Mathematical Methods for Digital Computers*; Ralston, A., Wilf, H. S., Eds.; Wiley: New York, 1960; pp 110–120.